THE EFFECT OF TEMPERATURE ON CORN STRAW ASH PRODUCTION AS SUPPLEMENTARY CEMENTITIOUS MATERIAL

ORIGINAL ARTICLE

PINHEIRO, Samantha Coelho[1], PAIVA, Otávio Augusto[2], OLIVEIRA, Mateus Ferreira de[3], SOARES, Gustavo de Albuquerque[4], RODRIGUES, Vitória Kethelen Monteiro[5], RIBAS, Luciane Farias[6]

PINHEIRO, Samantha Coelho. *et al.* **The effect of temperature on corn straw ash production as supplementary cementitious material**. Revista Científica Multidisciplinar Núcleo do Conhecimento. Year. 08, Ed. 09, Vol. 03, pp. 76-112. September 2023. ISSN: 2448-0959, Access link: https://www.nucleodoconhecimento.com.br/civil-engineering/corn-straw-ash, DOI: 10.32749/nucleodoconhecimento.com.br/civil-engineering/corn-straw-ash

1. INTRODUCTION

The civil construction sector is growing, which is of great socioeconomic importance. However, this increase has consequences that are already the focus of studies for many researchers. One of the main materials used in civil construction, cement, is responsible for a significant amount of carbon dioxide (CO_2) emissions. Cement production alone has been responsible for approximately 8% of global CO_2 emissions, primarily due to its high level of embodied carbon in cement factories (Blois; Lay-Ekuakille, 2021; Cadavid-Giraldo; Velez-Gallego; Restrepo-Boland, 2020 e Un Environment and International Energy Agency, 2017). Most of the CO_2 emissions come from burning the clinker used to produce this filler, along with the significant energy consumption required for this process. Cement factories, in addition to this, are responsible for the rapid consumption and depletion of limited resources.

In this way, it is important to conduct research that focuses on carbon-neutral construction and the utilization or recycling of materials that can decrease the consumption of finite resources. This research should also explore alternatives to

Ordinary Portland Cement (OPC) to protect the environment (Danish; Ulucak, 2020; Mota *et al*., 2017).

One way that has been gaining prominence is the incorporation of Supplementary Cementitious Materials (SCM) to reduce the use of clinker. This demonstrates that it is possible to use alternative cementitious materials for the production of OPC and maintain efficiency and meeting the necessary demand for the construction industry (Martirena; Monzó, 2018; Mo *et al*., 2016). The ashes from biomass residues are an example of SCM, as they are rich in silica and have been studied to better understand their behavior when incorporated into cementitious matrices in pastes, mortars, and concretes. Some examples of these ashes include rice husk ashes, elephant grass ash, and sugarcane bagasse ash, among others (Agwa *et al*., 2022; Cordeiro; Sales, 2016; Cordeiro; Toledo Filho; Fairbairn, 2009).

The agroindustry generates a significant amount of residual biomass from harvesting and processing, which poses a problem that needs to be solved. In the time period from 2000/01 to 2021/22, corn production increased from 591 million tons to 1.189 billion tons, with the United States, China, and Brazil being the top producers, and this increase is due to the high annual yield and great harvest potential (CONAB, 2023; Kang *et al*., 2020; Statista, [s.d.]). The main by-products that the corn crop leaves in the field are the leaves and stems, while in the industry, the cobs are produced. Corn straw commonly does not have a defined final destination, as it is generated during harvesting and becomes an agro-industrial waste. Both straw and cob are often stacked randomly, discarded, used as fertilizers, or used as fuel for daily use (Aliu *et al*., 2023; Chu *et al*., 2012; Zeng; Ma; Ma, 2007; Zhou *et al*., 2022). However, even in the latter case, waste is still generated in the form of ash and, in this context, this ash may have a pozzolanic character, react with the calcium hydroxide in the cement and form more hydrated calcium silicate (Abdalla; Ghafor; Mohammed, 2019; R. G. De Azevedo *et al*., 2022).

In recent years, research has focused on the use of corn straw for bioconversion into fuel ethanol, which brings both economic value and ecological benefits (Jin *et al*., 2017; Mengi-Dinçer; Ediger; Yesevi, 2021; Wang *et al*., 2021; Zhao *et al*., 2020). Even so,

there are some factors that pose a crucial challenge in the sugar conversion process, making it difficult to produce and reuse corn straw (Anca-Couce; Hochenauer; Scharler, 2021; Pino *et al*., 2018).

The residues mentioned above from the corn crop have the potential to produce a substantial amount of ash. This ash can possess a high pozzolanic capacity due to the high amount of silica, which promotes the reaction with calcium hydroxide (Qi; Feng; Wang, 2020; Qudoos *et al*., 2019). when obtained through a controlled burning process (Theng *et al*., 2015; Titiloye; Abu Bakar; Odetoye, 2013; Zhao *et al*., 2023), as well as reducing problems caused by floating pollution or land accumulation.

In this study, researchers such as Cordeiro *et al*. (2020) and Lima and Cordeiro (2021) conducted studies on the production of ash from corn straw (CSA). They evaluated the pozzolanic behavior of ash obtained at different temperatures and through controlled acid leaching. Additionally, they examined the compressive strength of mortars made with varying amounts of CSA as a replacement for OPC. The results were promising, indicating that CSA can be classified as a pozzolanic material with sufficient mechanical strength.

The significance of addressing agro-industrial residues is evident, as well as the potential for studying their integration into civil construction. This research contributes to the field by exploring the use of corn straw as a pozzolanic Supplementary Cementitious Material (SCM), which is a topic that has been sparsely covered in the literature. By doing so, it aims to address the aforementioned issues and reduce associated problems.

2 MATERIALS AND METHODS

2.1 MATERIALS

The corn straw required for the research was obtained from a distributor in a market in Manaus (state of Amazonas, Brazil). In this establishment, only corn derivatives are prepared, while the corn cobs and straws are discarded. Subsequently, the collected

material underwent a cleaning process to remove materials that were not relevant to the research. The hydraulic binder used was ordinary Portland cement, obtained without addition, obtained from local shops in the city of Manaus. Water from the city's water supply system and a superplasticizer composed of polycarboxylic ether (with a specific mass of 1.07 g/cm³ and an average solid content of 31.52%) were used to mold the pastes.

2.2 EXPERIMENTAL METHODS

2.2.1 PREPARATION OF BIOMASS SAMPLES AND ASH PRODUCTION

After being collected, the corn straw underwent initial cleaning to remove unwanted materials, such as the cob and corn stigma. These were sun-dried to remove surface moisture and subsequently dried in an oven at 105 ± 5 °C to eliminate any remaining moisture until a consistent mass was achieved. The biomass grinding procedure started with a branch crusher to reduce the size of the straws into smaller particles. This facilitates the burning process because a larger contact surface area improves the burning efficiency. However, the desired size was not achieved, and it was necessary to use a knife mill with a granulometric mesh that had an approximate opening diameter of 2.3 mm. This process resulted in the material particles being left in a suitable size for combustion.

The firing process was carried out in a muffle furnace equipped with a controller and a porcelain capsule for storing the material to be fired. Initially, the amount of material to be calcined was determined based on the sample mass and muffle volume ratio of 0.036, as established in the study by Cordeiro, Toledo Filho and Fairbairn (2009). This fixed proportion was adopted to maintain a uniform ratio between the mass of the straw and the volume of the internal chamber.

After weighing, the material was distributed into porcelain crucibles to maximize the available contact surface and ensure uniform burning. The firing procedure was conducted at five different firing temperatures, following the parameters outlined in the

work by Cordeiro, Toledo Filho and Fairbairn (2009). The heating rate used was 10 °C/min. First, the corn straw was burned at a temperature of 350 °C for three hours. Then, the temperature was gradually increased to the desired values of 400°C, 500°C, 600°C, 700°C, and 800°C, with each temperature being maintained for an additional three hours.

The material was burned, according to the aforementioned methodology, in a sufficient quantity to conduct the CSA characterization tests and for the production of cement pastes. To determine which burning temperature was more reactive, we used criteria such as the chemical and mineralogical composition, as well as other parameters including electrical conductivity, Chapelle pozzolanic activity index, loss on ignition, and ultrafine grinding. After obtaining the ashes, the CSAs were ground for homogenization. This step was necessary because the size of the CSAs varies with the increase in temperature, as observed by Barroso (2011) and confirmed during the collection of ashes in this study.

The samples were subjected to the milling process for 30 minutes, with the intention of achieving an average size (D50) of around 20 µm. The milling procedure was carried out in a high-energy ball mill (8000M Mixer/Mill®). The balls used in the milling process were made of steel and had a diameter of approximately 8.5 mm.

It was also necessary to determine the quantity of material that would be used during each milling process. The grinding of the ash had the following relationship: (i) use of steel balls, comprising 40% of the mass, relative to the volume of the cylinder; and (ii) adding a sample that accounted for 50% of the mass of the spheres. This same methodology was also used by Pinheiro (2015) and Paiva (2016) when grinding rice husk ash and sugarcane bagasse ash, respectively.

2.2.2 ASH CHARACTERIZATION

The chemical composition of the samples, in terms of oxides, was determined in an energy dispersive X-ray fluorescence spectrometer (EDXRF), EDX – 720 from Shimadzu. The fire loss of CSAs was carried out based on NBR NM 1836, weighing

1.000 g ± 0.001 g of CSA sample, calcined at a rate of 10 °C/min in a muffle furnace, at a temperature of 950 ± 50°C for approximately 50 min.

The crystalline phases present in the CSA, as well as the mineralogical composition, were identified using a Bruker diffractometer, model D2 Phaser. The radiation was operated at 40 kV and 30 mA, which was copper monochromatic (Cu Kα, λ = 1.5418Å), with an angle step of 0.02° and measurement interval between the Bragg angles (2Θ) of 10° and 80°. Diffraction patterns provided by the Inorganic Crystal Structure Database (ICSD) were used for the analysis.

With the ground ash in hand, the particle size distribution was determined using a Malvern Mastersizer laser particle analyzer, equipped with a Hydro 2000MU wet reading unit. The ash being tested was added to the system while maintaining the obscuration range, which is a measure of turbidity, between 10% and 20%. The Fraunhofer model was used due to the lack of a refractive index for the material. The pump was set to 2500 rpm and the ultrasound was set to level 3.0 for the first 30 s and 60 s after the final reading. This was done to analyze whether the material showed adequate dispersion.

For the analysis of specific surface area, a Micromeritics nitrogen analyzer, ASAP 2020, was used. The ash samples were pre-treated for 24 hours at 150°C under vacuum. Adsorption and desorption analyses were carried out at -196°C, using relative pressures ranging from 0.01 to 0.99 and a sample mass of approximately 0.3 g. The specific surface area was determined using the BET method (Brunauer-Emmett-Teller), while the Pore volume (Pv) and pore diameter (Pd) were calculated using the BJH method (Barrett-Joyner-Halenda) of desorption.

2.2.3 POZZOLANIC ACTIVITY

The pozzolanicity of the CSAs was verified through two analyses. First, the electrical conductivity method proposed by Luxán *et al*.(1989). To measure the electrical conductivity, a saturated solution of calcium hydroxide was used at a temperature of 40 ºC ± 1ºC. The ash to be tested, weighing 1.75 g, was immersed in the solution.

Temperature and readings were continuously monitored using the Multiparameters Labquest 2 equipment for 20 minutes. The authors propose that the minimum time required to verify pozzolanic activity is 2 minutes. Table 1 lists the classifications established by Luxán; Madruga and Saavedra (1989) regarding the material and its pozzolanic properties.

Table 1 – Evaluation of pozzolanic activity by measuring conductivity

Classification of the material	Variation of electrical conductivity (mS/cm) – 2 min
Non-pozzolanic	$\Delta C < 0.4$
Moderate pozzolanicity	$0.4 < \Delta C < 1.2$
Good pozzolanicity	$\Delta C > 1.2$

Source: Adapted from, Luxan et al. (1989).

The second method performed for pozzolanic analysis was the modified Chapelle method, as prescribed by NBR 15895 (ABNT, 2010). To carry out the experiment, 2.00 g of CaO and 1.00 g of the ash to be tested were added to an Erlenmeyer with a lid, along with 250.00 g of deionized water. The set was kept in a water bath at a constant temperature of 90°C ± 5°C for about 16 ± 1 h. After this period, the contents were added to a sucrose solution. Finally, the solution was titrated with HCl to determine the Chapelle pozzolanic activity index, mg of $Ca(OH)_2$ per g of material.

2.2.4 PRODUCTION OF PASTES BASED ON CEMENT AND CORN STRAW ASH

To assess the reaction of the ash with the cement, pastes were prepared using the most reactive CSA, as determined by the tests described in the ash characterization section. Initially, reference pastes (REF) were made using OPC-type cement with a water/cement ratio of 0.43. The ash pastes contained 10% cement replacement by mass (CSA-10%). The water-to-cementitious material ratio was maintained at 0.40, and specific superplasticizer contents were used to ensure consistent paste consistency within a spread diameter range of 100 ± 20 mm, as determined by the

Kantro minislump test (Kantro, 1980). For the REF and CSA-10% pastes, 0.10% and 0.16% of superplasticizer were used relative to the cement content, respectively.

The pastes were mixed in a 2-speed mixer using the following steps: (i) water + cement, kept at rest for 30 seconds; (ii) mixed at low speed for 30 seconds; (iii) scraped the bowl wall for 30 seconds; (iv) covered the mixture with a damp cloth and let it rest; and (v) blended the mixture on high speed for 120 seconds.

2.2.5 PASTE COMPRESSIVE STRENGTH

To determine the compressive strength of the paste made with the most reactive CSA, a total of 32 cylindrical specimens with dimensions of 25 mm in diameter and 50 mm in height were prepared and subjected to a uniaxial compression test. The specimens were cured in lime-saturated water at a temperature of 25°C, using the SL-155 thermostatic water bath. After curing for 7, 28, 56, and 91 days, the samples were faced at both ends on a lathe. The test was conducted using an Instron universal mechanical press equipped with a 150 kN load cell, and the loading speed was set at 0.1 mm/min.

2.2.6 TOTAL AND CAPILLARY ABSORPTION

Water absorption through total immersion and capillary are essential factors for assessing durability, as pastes, concrete, and mortars are exposed to weathering processes such as rain and direct contact with water containing aggressive agents. The total water absorption (A) was determined by NBR 9778 (ABNT, 2009). Additionally, the void index (Iv) was calculated, which indicates the volume of pores accessible to water under direct contact and without a gradient depression. The specific mass of the hardened cementitious paste (ρr) was also determined according to the methodology described in the standard after 28 and 91 days of curing. For the test, 12 specimens of 25 mm in diameter and 50 mm in height were molded. These specimens were previously immersed in water for 72 hours and then boiled for 5 h.

To determine the water absorption by capillary rise, the methodology outlined in NBR 9779 (ABNT, 2012) was used. For the test, the drying temperature of the specimens was adjusted to 60 °C. The test was carried out on 12 samples of pastes, measuring 25 mm in diameter and 50 mm in height, for the reference specimens and replacing 10% of CSA with cement.

3 RESULTS AND DISCUSSION

3.1 ASH CHARACTERIZATION

3.1.1 ASH YIELD

The average yield results obtained were 3.52, 2.87, 2.61, 2.33, and 2.26% for the ash obtaining temperatures at 400, 500, 600, 700, and 800 ºC, respectively. These results indicate that when carrying out the heat treatment with corn straw powder, the ash yield is considerably reduced due to the amount of organic matter in it. Yields also vary according to the fineness of the sample after grinding, as well as the moisture content in the straw. Therefore, the result is subject to change.

Cordeiro *et al*. (2020) conducted a study on the leaching of rice husk, corn straw, and bamboo leaves with the aim of producing pozzolanic ash. Because of this, the authors chose to conduct a pre-burning stage on these materials. This stage simulated the burning process that takes place in the particulate collector in sugar and alcohol plants. The average yield achieved after this process was 22% by mass for rice ash, 13% for corn straw, and 23% for bamboo leaf. It should be noted that after the initial firing, the authors further subjected the sample to a muffle furnace for an additional 3 hours at 600°C. This step was intended to theoretically reduce the final yield even further.

3.1.2 PARTICLE SIZE DISTRIBUTION OF THE CSA

Fig. 1 shows the granulometric curves of the OPC and the CSAs calcined at the five firing temperatures and after grinding for 30 min. The ashes were ground to minimize

RC: 148586
Available in: https://www.nucleodoconhecimento.com.br/civil-engineering/corn-straw-ash

the size of the particles. Through the curves, it can be seen that the milling process resulted in a finer particle size distribution as the milling time increased.

Fig. 1 – Particle size distribution curves obtained for OPC and ground CSAs

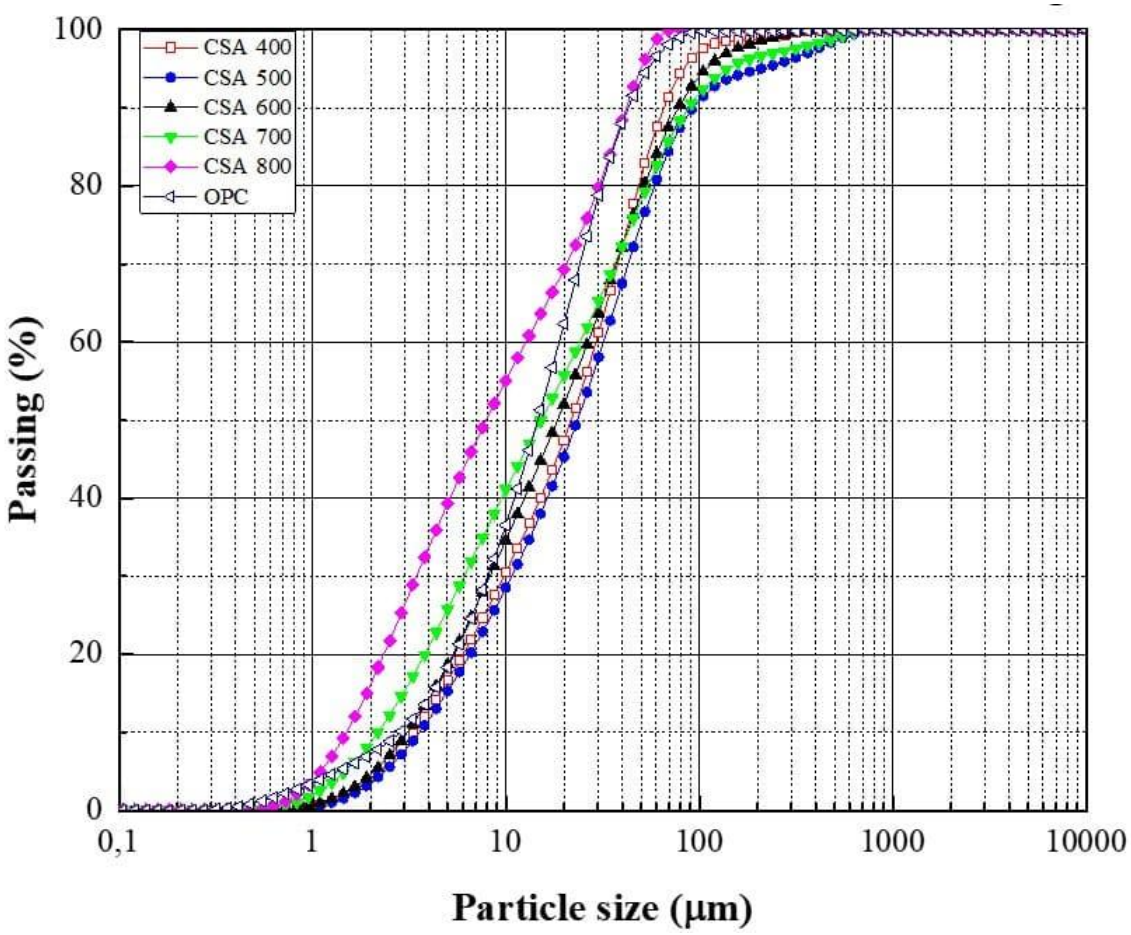

Source: Own authorship (2023).

Table 2 lists the values of D10, D50, and D90 obtained from the granulometric analysis.

The specific mass values obtained for each ash after milling are also listed in this table. It should be noted that parameters D10 and D90 refer to the cut diameters of the cumulative distribution curve at 10% and 90%, respectively, while parameter D50 represents the average particle size.

Table 2 – Characteristics of particle size and specific mass for OPC and ground CSAs

Samples/variables	CSA 400	CSA 500	CSA 600	CSA 700	CSA 800	OPC
D_{10} (µm)	2.913	3.116	2.704	1.905	1.3	2.471
D_{50} (µm)	18.965	20.426	16.115	13.234	6.89	12.739
D_{90} (µm)	57.014	80.591	67.693	76.436	36.44	37.338
Specific mass (g/cm³)	2.109	2.256	2.303	2.387	2.465	3.179

Source: Own authorship (2023).

Through the values in Table 2 and Fig. 1, it can be seen that as the corn straw calcination temperature increased, the particles had a reduction in D50, varying between 6 and 20 µm. Cordeiro *et al*. (2020) when grinding for 30 minutes, in a high energy mill (Union Process), the CSA leached with citric acid, reached a D50 of 6.8 µm, while Lima and Cordeiro (2021) when performing the CSA grinding, for 30 minutes and also in a high energy mill, they obtained a D50 of 9.23 µm. The last authors, when substituting cement for CSA (without chemical treatment), concluded that it does not decrease the compressive strength of mortars when the substitution content varies between 10% and 30%. Therefore, from the dimensions of the CSAs reached in this research, the CSAs 700°C and 800°C are those that are close to the dimensional range found by the aforementioned authors and can be used for experimental tests to analyze their potential as mineral addition.

As for the specific mass of the CSAs produced, it is noted that as the temperature increases, the specific mass tends to grow, due to the CSA becoming more crystalline with the rise in the firing temperature. Through Table 2, it can be seen that the specific mass values varied between 2.109 and 2.465 g/cm³, approaching the value of 2.36 g/cm³ found by Lima and Cordeiro (2021) for the CSA produced without chemical treatment.

3.1.3 CHEMICAL COMPOSITION

Depending on the quantitative analysis of the elements performed by EDXRF, the chemical composition of OPC (Table 3) and ground corn straw and the CSAs for the

five temperatures (Table 4) were obtained. Tables 3 and 4 present the percentages of chemical elements in oxides, along with the percentages of loss on ignition of the various ashes. These values demonstrated a decrease as the temperature of ash production increased.

Table 3 – Oxide composition and loss on ignition of OPC

Oxides	Cimento CP I (%)
CaO	69.17
SiO_2	15.01
Fe_2O_3	5.51
Al_2O_3	4.56
SO_3	4.55
K_2O	0.53
TiO_2	0.33
MnO	0.26
SrO	0.05
CuO	0.02
ZnO	0.02
$SiO_2+Al_2O_3+Fe_2O_3$	25.08
Loss on ignition	-

Source: Own authorship (2023).

RC: 148586
Available in: https://www.nucleodoconhecimento.com.br/civil-engineering/corn-straw-ash

Table 4 – Oxide composition and loss on ignition of corn straw in natura and

Oxide	Corn straw in natura (%)	400°C (%)	500°C (%)	600°C (%)	700°C (%)	800°C (%)
K_2O	51.00	29.27	30.15	33.18	33.10	32.28
SiO_2	19.71	25.32	27.15	31.14	33.65	36.99
P_2O_5	9.01	8.05	7.87	8.77	10.33	11.40
Fe_2O_3	1.25	4.22	2.59	2.24	1.50	1.42
CaO	4.70	4.12	4.66	4.47	5.76	6.14
SO_3	13.88	2.96	3.14	3.63	3.93	4.07
ZnO	0.45	0.24	0.23	0.26	0.28	0.29
Others	-	0.83	0.54	0.69	0.54	0.70
SiO_2+Al_2O3+Fe_2O_3	20.96	29.54	29.74	33.38	35.14	38.41
Loss on ignition	-	25.00	23.68	15.62	10.91	6.71

Source: Own authorship (2023).

With regard to the composition of the OPC, it is confirmed that it complies with the chemical requirements required for Portland cement according to NBR 16697 (ABNT, 2018), in which the MgO and SO3 content are below 6.5% and 4.5%, respectively, and the loss on ignition is less than 4.5%. It is also verified that the CSAs presented several chemical elements, in a more abundant way K, Si and P, and lesser amount of Fe, Ca, S and Zn. It should be noted that the levels of K, P and Ca are a result of the corn fertilization process carried out in the state of Amazonas. In the preparation of the soil, organic matter and limestone are incorporated to correct acidity and improve soil quality. Oliveira *et al*. (2018) point out that the adequacy of soil fertility in the state, to achieve high corn productivity, is carried out through the insertion of macronutrients (nitrogen, phosphorus and potassium) and the correction of acidity (liming).

When comparing the results of Table 4 with the recommendations of Table 5, it is evident that the ashes produced for the five temperatures, according to classification E, have: (i) sum of SiO_2 + Al_2O_3 + Fe_2O_3 less than 50%; (ii) SO_3 values below the established limit, which is 5%; and (iii) Loss on Ignition greater than 6%. Therefore, due to these two unmet requirements, it is not possible to infer that ash is considered Class E (ABNT, 2014).

Table 5 – Chemical requirements (ABNT, 2014)

Properties	Pozzolanic material class		
	N	C	E
$SiO_2 + Al_2O_3 + Fe_2O_3$ (%)	≥ 70	≥ 70	≥ 70
SO_3 (%)	≤ 4	≤ 5	≤ 5
Moisture content (%)	≤ 3	≤ 3	≤ 3
Loss on ignition (%)	≤ 10	≤ 6	≤ 6
Alkalis available in Na_2O (%)	≤ 1.5	≤ 1.5	≤ 1.5

Source: Own authorship (2023).

According to Table 5, when analyzing the chemical composition of straw in natura and the CSAs, it is noted that the contents of K_2O, Fe_2O_3 and SO_3 decrease compared to the natural state. However, these levels show a slight increase with higher temperatures. Compounds such as P_2O_5, CaO, and SiO_2 showed increases of up to 26%, 30%, and 87%, respectively. It is noteworthy that the increase in the amount of Si and the consequent reduction of K are favorable. This allows the ash to partially replace the cement in mass, serving as a mineral addition.

According to Table 5, the presence of K was noted, an alkaline metal that can be harmful to the cement paste if present in large quantities, since it is responsible for the alkali-aggregate reaction, a chemical reaction between mineral forms of “unstable” silica with fine and/or coarse aggregates and the alkaline hydroxides (i.e. Na^+, K^+ and OH^-) that are dissolved in the concrete pore solution. This reaction generates a gel, which causes expansive pressure within the reacting aggregate materials and the adjacent cement paste when it absorbs moisture from the surrounding environment. As a result, microcracks may form, leading to a loss of material integrity (including mechanical properties and durability) and, in some cases, compromising the functionality of the affected structure or structural member (De Grazia *et al*., 2021).

Comparing the chemical compositions of the CSA, in oxides, listed in this work with those of Lima and Cordeiro (2021), it is evident that the authors, when producing CSA at a temperature of up to 650 °C, approximately, found SiO_2 values of up to 62.5%, in addition to K_2O contents of 17.2% and 8.7% of CaO. The authors also found Fe, S, P, Mn and Ti oxide contents, however, in small amounts. It should be noted that due to the type of soil in the Amazon, the values of the chemical composition of the work by Lima and Cordeiro (2021) in relation to this vary, however, the chemical elements are the same.

In a similar manner, other authors also analyzed the chemical composition of the ashes produced from corn straw. Xu *et al*. (2021) found that the oxides present were mainly Si (37.03%), followed by Ca (16.71%), Mg (16.70%) and K (12.93%). Perná *et al*. (2019) used the CSA obtained from a heating plant in the Czech Republic. However, the CSA it had a high carbon content of 31.51%, in its composition, which was reflected in low levels of oxides, the most abundant being K (25.39%), Si (11.76%), and S (11.55%). Niu *et al*. (2019) when studying the CSA of biomass from China, obtained Si (29.30%), K (28.50%), Ca (15.40%), and Mg (9.98%) as the main oxides. Yao *et al*.49 calcined, at 575 °C, biochar residues from the gasification of different biomasses, obtained in China, one of which was CSA, whose composition mainly presented oxides of Si (47.28%), K (17.65%), and Ca (12.45 %).

Given the results above, it is stated that the chemical composition of each CSA produced varies depending on several factors. These factors include the burning temperature, the calcination process (whether obtained in a plant or in a muffle furnace with controlled burning), and the location where the agricultural crop is planted. It is important to note that the soil also plays a significant role in influencing the chemical composition of the plant. Even so, it is possible to verify that, despite the varying oxide contents, the most abundant ones are SiO_2, K_2O, and CaO, coinciding with those shown in the analysis of the CSA referring to this work, as listed in Table 5.

RC: 148586
Available in: https://www.nucleodoconhecimento.com.br/civil-engineering/corn-straw-ash

3.1.4 MINERALOGICAL COMPOSITION

Fig. 2 illustrates the crystalline compounds present in the ash produced after 30 minutes of grinding and identified by X-ray diffraction. The XRD images below show the ash produced at burning temperatures of 400°C, 500°C, 600°C, 700°C, and 800 °C. The results indicate that the peaks corresponding to quartz (SiO_2), sylvite (KCl) and arcanite (K_2SO_4) could be found in each spectrum, however, due to variations in firing temperatures, these peaks had their intensities altered as they increased. It is also noteworthy that at CSA 800°C, the formation of cristobalite (SiO_2) was observed.

Fig. 2 – X-ray diffractograms of corn straw ash

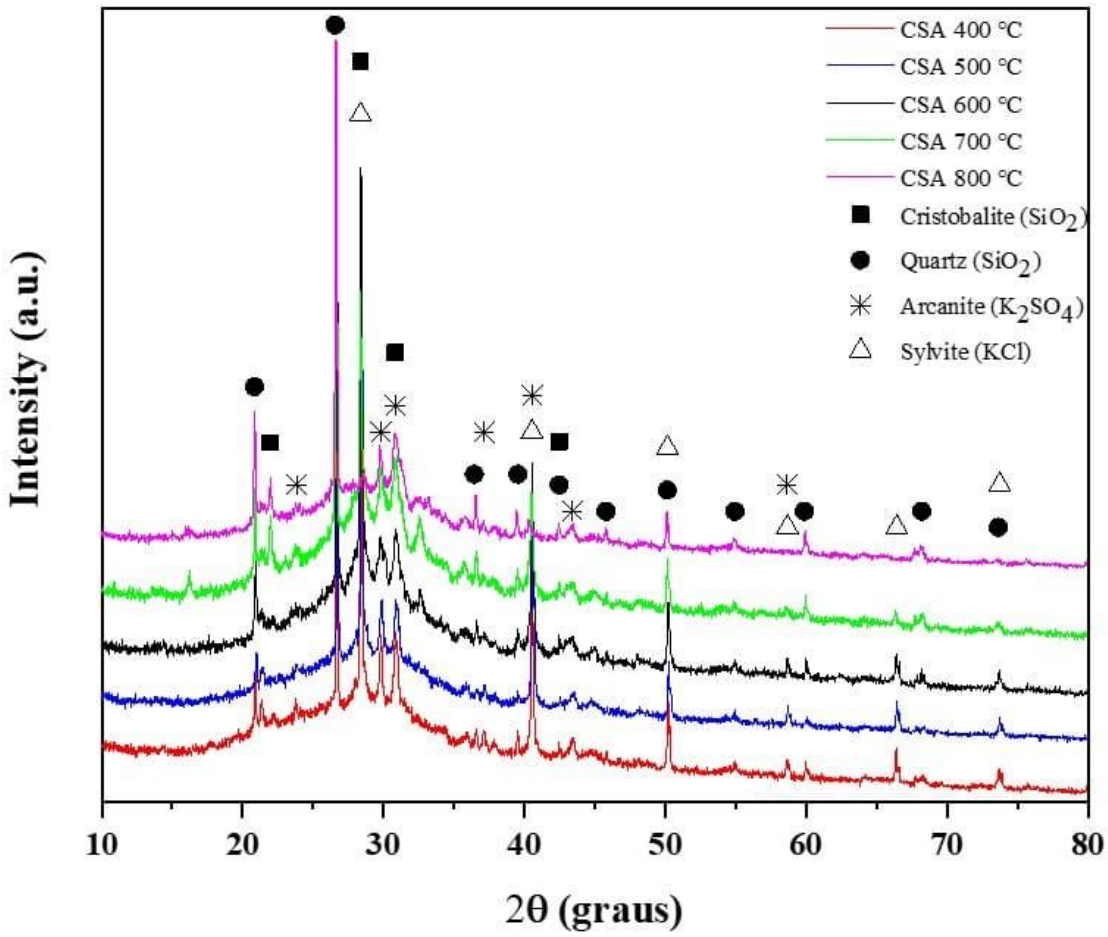

Source: Own authorship (2023).

As shown in the image above, the presence of crystalline silica is evident, in the form of quartz (ICSD 16331) and cristobalite (ICSD 77452), with the peaks of the latter being

better defined and pronounced in the diffractogram at 800 °C, which can be attributed to the high firing temperature. It should be noted that there is a deviation from the baseline, verified between the Bragg angles of 20° and 40°, indicating the presence of silica in the amorphous state. Sylvite peaks (ICSD 165593) were also found, more intensely at temperatures from 400 °C to 700 °C. Additionally, arcanite peaks (ICSD 79777) were detected. Such minerals and an amorphous halo were also observed in the works of Lima and Cordeiro (2021), Cordeiro *et al*. (2020), Perná *et al*. (2019) and Niu *et al*. (2019) when analyzing corn straw ash. Still, Capablo *et al*. (2009) when studying corn straw ash, found high amounts of potassium oxide, in addition to calcium oxide, sulfur and phosphorus, proving the presence of sylvite and arcanite.

Through Fig. 2, it can be verified that when increasing the firing temperature, the quartz peaks had their intensities increased as the sylvite peaks were reduced. This phenomenon was also reported by Shakouri *et al*.51 when analyzing the XRD pattern of corn cob ash, produced at temperatures ranging between 600°C and 700°C, in addition to showing amorphous content between positions 25° and 35°, the authors also identified sylvite as the main crystalline phase, since the melting point of KCl is 770°C.

Existing forms of potassium-bearing compounds in ash exert influence on ash melting because alkali metals can promote the formation of low-temperature eutectics (Yao *et al*., 2020). Anicic *et al*. (2018) indicated that potassium can be easily released by vaporization and transformed into gaseous/aerosol phases or retained in ash. This process leads to the formation of K2SO4, generated as a product of potassium sulfation. Additionally, KCl is formed by the combination of K+ and Cl- radicals released in biomass combustion. Yao, Xu and Liang (2017) also certify that at higher incineration temperatures, less sylvite can be expected due to the reaction of KCl with SiO_2, Al_2O_3, and residual phases of potassium aluminosilicate, resulting in the release of HCl.

3.1.5 SPECIFIC SURFACE AREA (BET)

Table 6 presents the values of specific surface area determined by the BET method, as well as the Pore volume (Pv) and Pore diameter (Pd) obtained using the BJH

method. According to what was found, CSA milling for 30 minutes resulted in an increase in the BET specific surface area. The highest increase was observed for CSA 500, with a value of 7757.20 m²/kg. Additionally, the Pd was measured at 11.17 nm and Pv at 0.025 cm³/g.

Table 6 – Characteristics obtained for CSA 700 °C after nitrogen physisorption

Samples	BET specific surface area (m²/kg)	Pore diameter (nm)	Pore Volume (cm³/g)
CSA 400	4490.90 ± 60,00	11.17	0.025
CSA 500	7757.20 ± 11,75	8.54	0.035
CSA 600	3755.2 ± 7,75	20.85	0.028
CSA 700	1927.0 ± 5,35	32.64	0.017
CSA 800	1839.8 ± 5,23	24.91	0.013

Source: Own authorship (2023).

According to the table above, the surface areas varied in the range between 1839.80 and 7757.20 m²/kg, indicating not only similar BET values but also comparable pore volumes. These less expressive BET variable values are attributed to the presence of quartz content in the ash of the corn straw produced (Fig. 2). Additionally, the levels of other contaminants, such as carbon content, present in the samples contribute to this phenomenon (Barbosa; Cordeiro, 2021). When comparing the results, it is noted that the CSA 800 has the lowest BET value and, consequently, the highest silica content (Table 5) and other minerals resulting from the crystallization of burnt ash at 800°C (Fig. 2). This result is further confirmed by the lowest pore value of the sample, 0.013 cm³/g. According to Table 6, when examining the pore diameter values, it is confirmed that they are in the range of 2 and 50 nm, which classifies them as mesoporous according to IUPAC (Everett; Butterworths, 1972).

Through nitrogen physisorption of the CSAs produced, it was also possible to obtain the nitrogen adsorption-desorption isotherms of all firing temperatures, as shown in Fig. 3. The graphs below depict similar trends and, in accordance with the IUPAC (Everett; Butterworths, 1972) classification, all ash isotherms were said to belong to type V with hysteresis material H3, characterizing them as mesoporous solids, with the presence of uniform and non-uniform pores. Sing *et al*. (1985) complement these results by mentioning that H3 hysteresis is typical of narrow pores in the form of slits.

Fig. 3 – Nitrogen adsorption-desorption isotherms for: a) CSA 400; b) CSA 500; c) CSA 600; d) CSA 700; and e) CSA 800

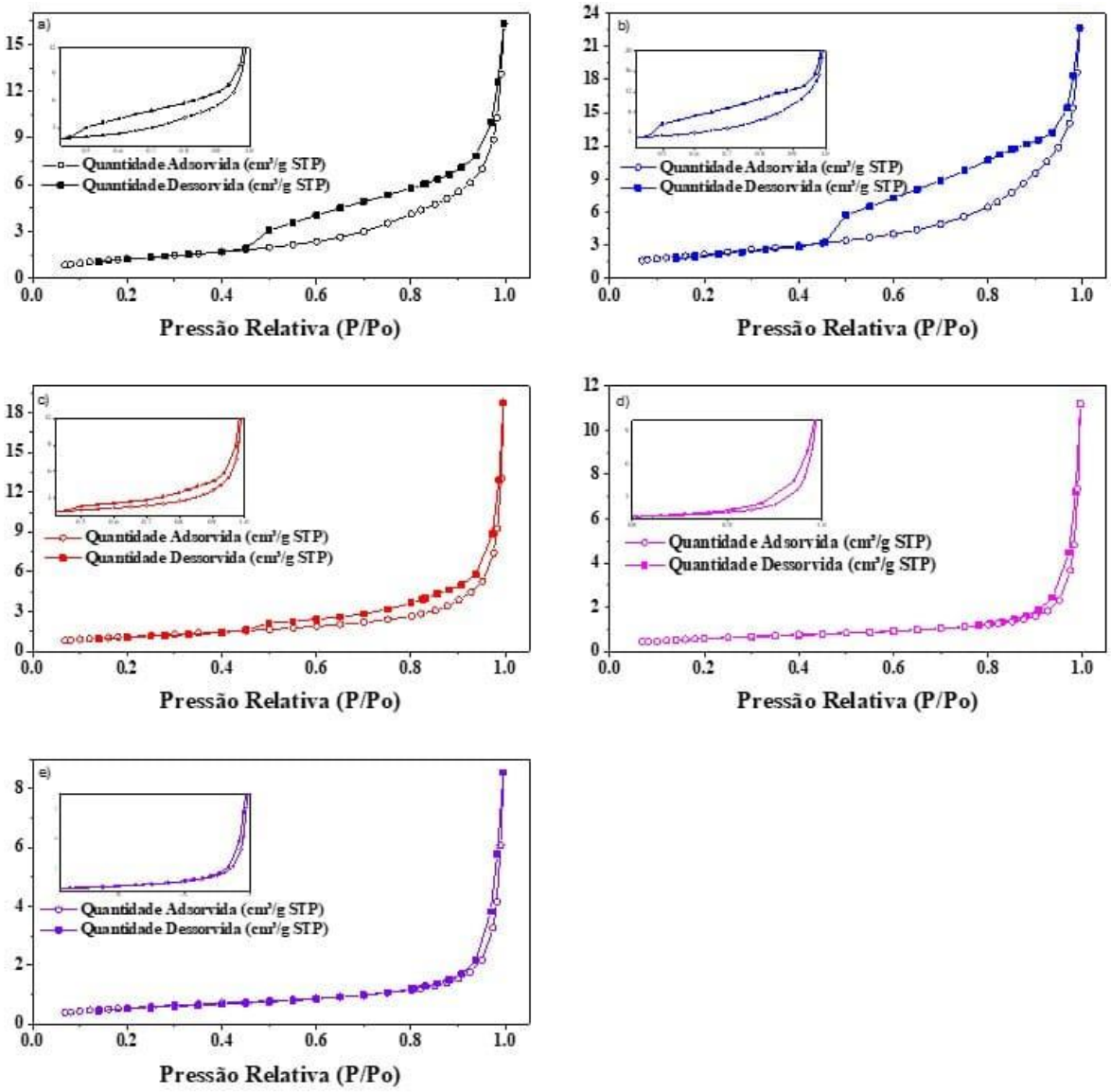

Source: Own authorship (2023).

Through the Fig. 3 above, it can be observed that hysteresis can be visualized in the values of relative pressure (P/Po) ranging from 0.42 to 1.0 for CSA 400, 500, and 600; and from 0.8 and 1.0 for CSA 700 to 800. Curves with hysteresis of type H3 were also reported by Barbosa and Cordeiro (2021) and Vieira *et al*. (2020) when studying sugarcane bagasse ash and rice husk ash, respectively. Referring to the study conducted by Barbosa and Cordeiro (2021), for SCBA 1, the authors found a surface area of 5500 m²/kg and a pore volume of 0.013 cm³/g. This fact was due to SCBA 1

containing a significant amount of crystalline silica, in the form of quartz, which also contributed to reducing the pore volume.

According to the results obtained from the characterization of the ashes, the CSA produced at 700°C exhibited the best characteristics. This particular ash had a higher sum of Si, Fe, and Al oxides compared to the other ashes. Additionally, its mineralogical composition was less crystalline compared to the CSA produced at 800 °C, which contributed to its reactivity. Furthermore, it showed the highest value of the Chapelle pozzolanic activity index. In addition, upon observing the granulometric curve, it is noted that CSA 700°C presented a D50 value less than 20 µm, which contributed to its selection.

3.2 POZZOLANIC ACTIVITY

3.2.1 ELECTRICAL CONDUCTIVITY

This analysis was carried out for the CSA ground for 30 minutes, as seen in the granulometric analysis. Through Fig. 4a, it can be seen that the ashes produced exhibited an increase in electrical conductivity values within the first reading range, followed by some stability or a slight decrease. Due to this initial increase in conductivity, the CSA presented a negative ΔC value, since the ashes contain alkaline oxides, such as K2O and CaO.

RC: 148586
Available in: https://www.nucleodoconhecimento.com.br/civil-engineering/corn-straw-ash

Fig. 4 – Electrical conductivity curves: a) uncorrected; and b) corrected

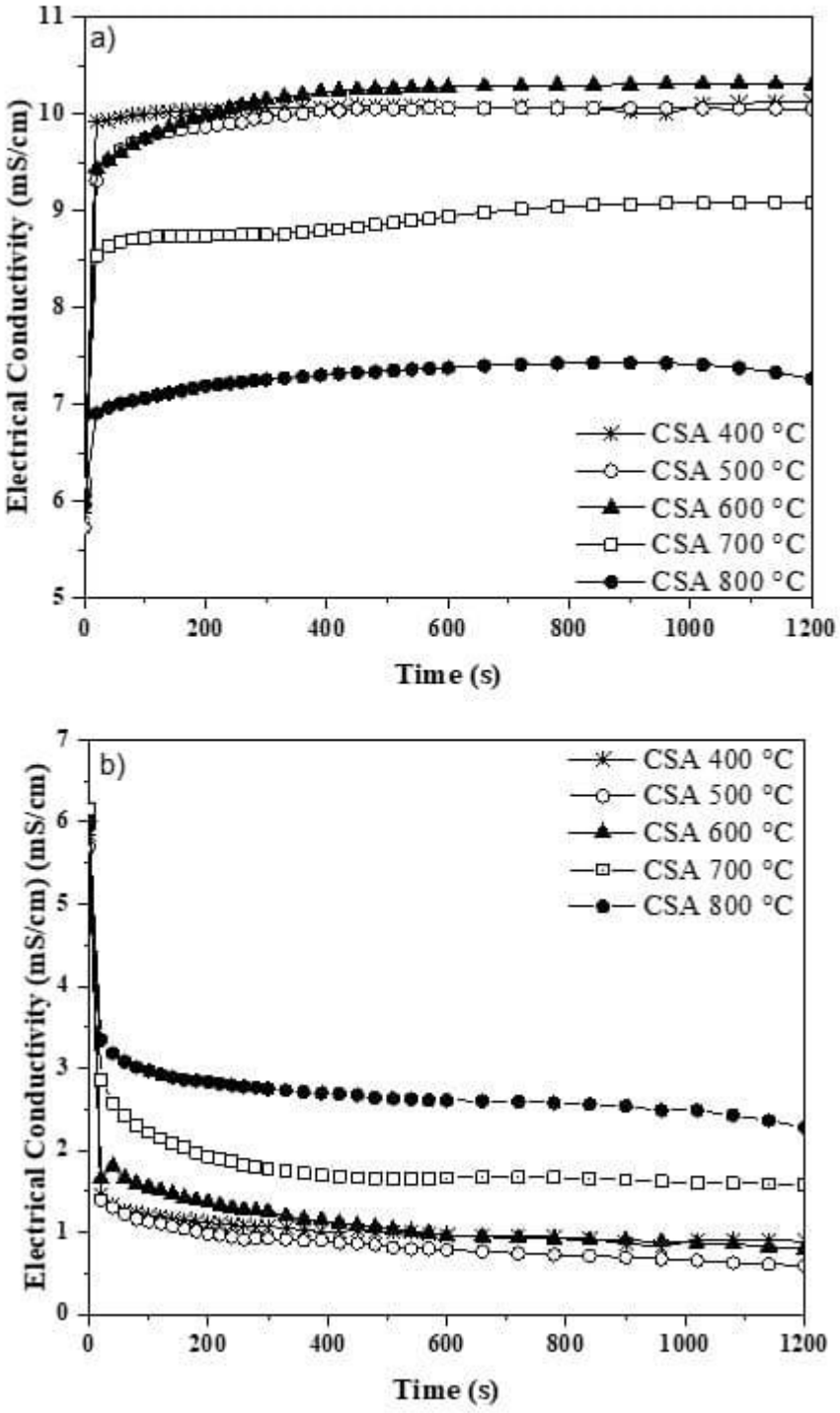

Source: Own authorship (2023).

Negative values of electrical conductivity were also found by Lima and Cordeiro (2021) when analyzing corn straw ash, produced at around 650 °C. Because of this, both the

authors mentioned here and this work performed an adaptation by subtracting the electrical conductivity values measured for the CSA immersed in a saturated solution of $Ca(OH)_2$ from the values of the CSA immersed in distilled water, as shown in Fig. 4b.

According to Fig. 4b, the corrected electrical conductivity curves decrease during the initial seconds of reading, but then remain relatively constant throughout the test duration. This effect occurred due to the consumption of calcium hydroxide by the ash, resulting in the formation of insoluble products through pozzolanic reactions. Table 7 lists the electrical conductivity values for the CSA produced at the 5 temperatures. It is observed that all ashes are classified as having good pozzolanicity, according to the classification established by Luxán, Madruga and Saavedra (1989).

Table 7 – Variation of electrical conductivity measured for CSA

Ash analyzed	ΔC (mS/cm)	Classification
CSA 400 °C	4.650	Good pozzolanicity
CSA 500 °C	4.585	
CSA 600 °C	4.559	
CSA 700 °C	4.005	
CSA 800 °C	3.023	

Source: Own authorship (2023).

Corroborating the results of good pozzolanicity found for CSA, Rolón and Castañeda (2021) obtained a ΔC of 1.175 mS/cm, indicating medium pozzolanicity, while Lima and Cordeiro (2021) and Cordeiro *et al*. (2020) found ΔC equivalent to 1.27 mS/cm and 3.73 mS/cm, respectively, suggesting that the ash exhibits good pozzolanicity. It should be mentioned here that in the first study, CSA was produced at 600 °C for one hour, while in the last two studies, the authors followed the same burning methodology to produce corn straw ash, with a temperature of up to 650 °C. It is also noteworthy

that Cordeiro *et al*. (2020) obtained a higher pozzolanic value by leaching the straw with citric acid. This was done to minimize the effect caused by alkaline metals present in the agricultural residue.

Compared to other ash derived from agricultural residues, the CSA produced in this work obtained ΔC values as high as the ash already studied and used as pozzolanic additions. Cordeiro *et al*. (2020) studied the effects of citric acid treatment on sugarcane bagasse ash (SBCA) and Rice Husk Ash (RHA). They obtained ΔC values of 0.74 mS/cm and 5.78 mS/cm, indicating average and good pozzolanicity results. While studying finely ground SBCA treated with hydrochloric acid, Barbosa and Cordeiro (2021) achieved a ΔC of 1.99 mS/cm, classifying it as gray with good pozzolanicity.

3.2.2 MODIFIED CHAPELLE TEST

The method for determining the fixed lime content was determined using the modified Chapelle. Therefore, this test was based on the consumption of portlandite by the ashes, allowing the establishment of quantitative data for comparison between them. Through this consumption, the maximum reactive potential of the mineral addition is verified. Fig. 5 shows the lime consumption, in mg $Ca(OH)_2$/g of ash, in each of the ground samples after 30 minutes.

RC: 148586
Available in: https://www.nucleodoconhecimento.com.br/civil-engineering/corn-straw-ash

Fig. 5 – Chapelle pozzolanic activity index results found for CSA

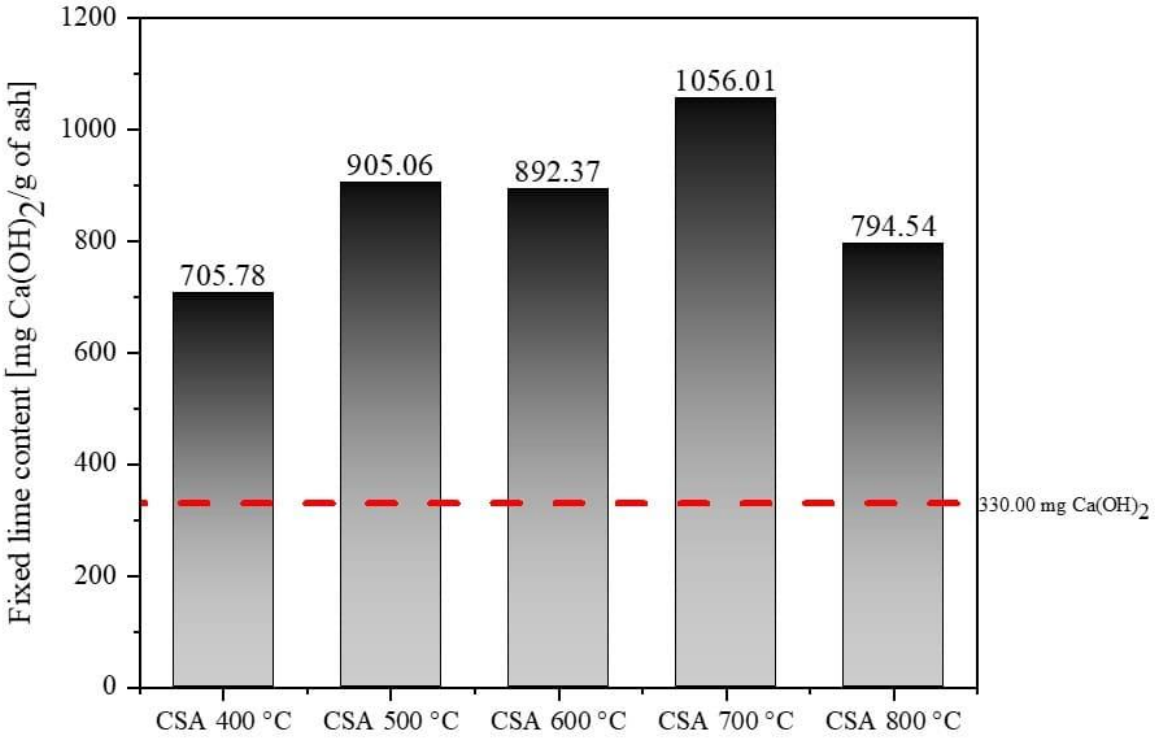

Source: Own authorship (2023).

Through the Fig. 5 above, it can be seen that the Chapelle pozzolanic activity index values obtained for the CSA tend to increase as the firing temperature is high, however, for the CSA at 800 °C, this value decreased abruptly. This behavior confirms what was demonstrated in the chemical and mineralogical compositions Through Table 5, it can be observed that the CSA decreases the amounts of alkali metals as the firing temperature increases from 400 °C to 700 °C. This decrease in alkali metals leads to an increase in the Chapelle pozzolanic activity index. The same does not happen for CSA 800 °C, as the mineralogical composition of this ash resembles crystalline minerals such as silica in the form of cristobalite, which reduces its reactivity. This contributes to the lowest value of Chapelle among the other ashes produced at this temperature.

Through Fig. 5, it is emphasized that all samples had a pozzolanic activity value greater than 330.00 mg $Ca(OH)_2$/g (Fig. 5 - red dashed line), which is the minimum value established by Raverdy *et al*. (1980) for a sample to be considered as pozzolanic.

When comparing the results obtained from the electrical conductivity test and the data presented in Fig. 5, it is evident that there is a correlation between the two. Both experiments carried out indicate that the ashes have good pozzolanic activity. However, unlike the electrical conductivity test, where the ΔC decreases as the CSA firing temperature increases, in the Chapelle pozzolanic activity index, the pozzolanic activity tends to increase as the CPM firing temperature increases. This was due to the amount of carbon present in the ashes, making the ΔC higher in CSA with a higher loss on ignition.

When comparing the results found in this research for the CSA with the works already carried out with ashes from agricultural residues, it is noted that the values found here are similar to those of ashes considered pozzolanic. Cordeiro and Sales (2016) produced elephant grass ash (EGA) at 600 °C, using the same firing conditions as in this work, finding a Chapelle value of 883 mg $Ca(OH)_2$/g and ΔC of 1.63 mS/cm. According to the work carried out by the authors, the sum of Si, Al, and Fe oxides was 84.40%, indicating that the ash possesses good pozzolanicity. By comparing the values obtained by the authors with those of this study, it is observed that the CSA, despite presenting the sum of these same oxides ranging from 29% to 40%, had Chapelle activity index values between 705.78 and 1056.01 mg $Ca(OH)_2$/g, indicating reactivity as high as the EGA.

In addition to the aforementioned work, other works that studied pozzolans that are widely disseminated also had values as high as those obtained for the CSA. Andrade Neto *et al*. (2021) analyzed the Chapelle pozzolanic activity index of SCBA and obtained values of up to 1023.96 mg $Ca(OH)_2$/g. Hasnain *et al*. (2021) studied RHA and observed values of 480.10 mg $Ca(OH)_2$/g and 412.05 mg $Ca(OH)_2$/g for SCBA and RHA, respectively.

3.3 PASTE COMPRESSIVE STRENGTH

Regarding spreadability, both the REF and CSA-10% pastes achieved values of 10 ± 2 cm, as specified. The REF paste had spreading values of 9.77 ± 0.12 cm, while the CSA-10% had values of 9.25 ± 0.11 cm.

RC: 148586
Available in: https://www.nucleodoconhecimento.com.br/civil-engineering/corn-straw-ash

The compressive strength results of the REF and CSA-10% pastes at 7, 28, 56, and 91 days of curing are shown in Fig. 6. The average of four samples was taken for each test age, and the error bars were added to the graph to indicate the dispersion of the results, which varied based on the breaking age and mixing of the paste. In general, all mixtures showed an increase in compressive strength values with the progression of hydration. The results show that the CSA-10% pastes achieved a higher initial strength gain after 7 days of curing, leading to improved performance.

Fig. 6 – Compression strength for REF and CSA-10% pastes

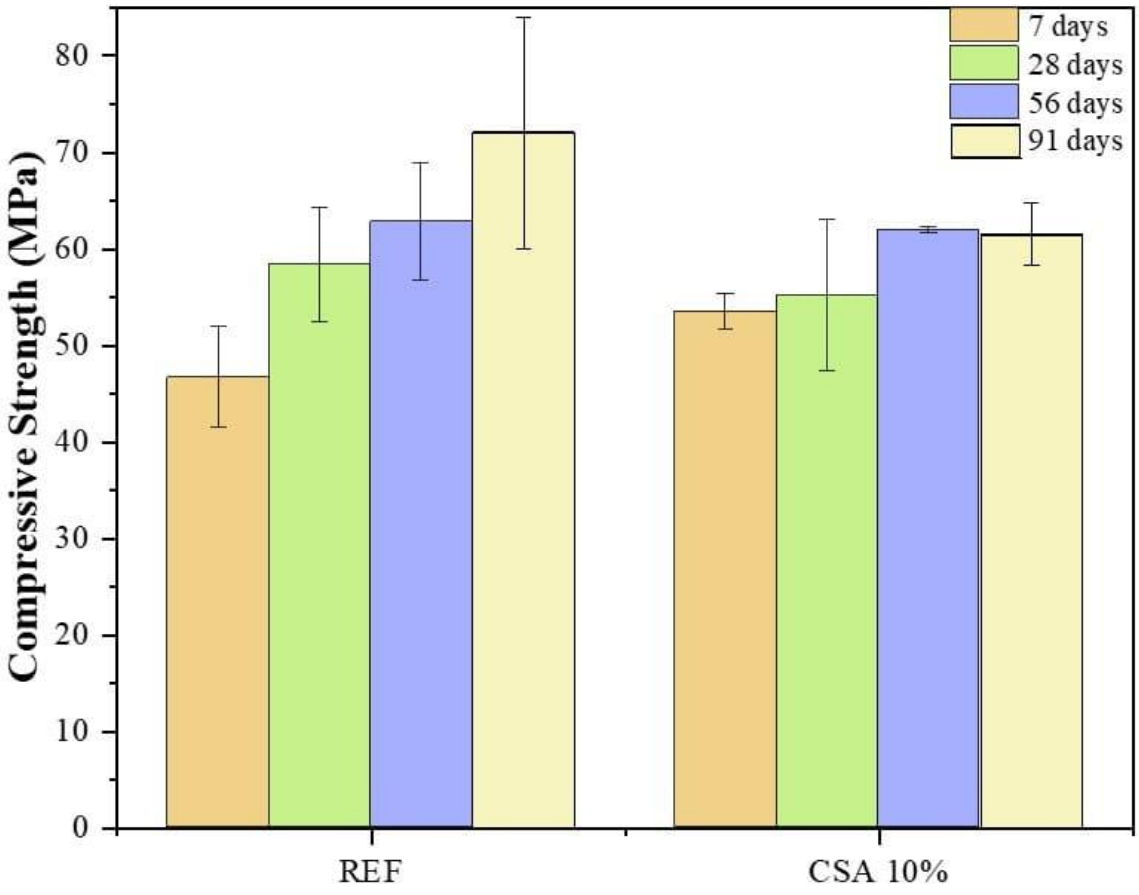

Source: Own authorship (2023).

However, since CSA 700 does not provide values for the combined content of iron, aluminum, and silicon oxides, as well as the loss on ignition content, close to the minimum of 50% and 6%, respectively, as standardized by NBR 12653(ABNT, 2014), the low pozzolanic activity of the ashes meant that there was no significant increase in

strength over time. It is noteworthy here that at 28 and 56 days, the compressive strength of CSA-10% was similar to that of REF, differing by about 5.42% and 1.37%, respectively.

It should be noted that the partial replacement of cement with ash led to a 0.06% increase in the dosage of superplasticizer in the pastes in the pastes. This factor was also observed by Lima and Cordeiro (2021) when producing pastes and mortars with CSA. The increase in superplasticizer required to adjust the consistency of the mix is directly proportional to the specific surface area of the ash and the content of cement replacement in each mix. Similarly to the results presented here, Raheem *et al*.(2017) found a reduction in compressive strength after 56 days compared to the result at 28 days. The authors hypothesized that this was due to the pozzolanic activity of the corn stalk ash, which could have created pores in the concrete and led to lower strength due to water evaporation.

Wang *et al*. (2021) observed that the uniaxial compressive strength increased when using corn straw ash to compose cemented coal gangue landfill. They noted that by increasing the replacement content of fly ash with CSA, the strength improved. They found that replacing up to 40% by weight of fly ash with CSA is the optimal amount for strength in all ages tested by the authors. This is because the coal gangue particles are tightly packed and the reaction products (CSH and ettringite) are denser and more durable.

Odeyemi *et al*. (2021) noted that there was a progressive increase in the compressive strength of concrete molded with a blend of corn straw ash and Palm Oil Fuel Ash (POFA) as the curing days increased. The optimal combination of ash percentages for replacing cement was found to be 30% POFA and 16.6% CSA.

Therefore, it appears that the development of strength at the specified curing age is associated with the level of CSA reactivity. However, it is not a concern if ash produced has low reactivity, as CSA can still contribute to the strength performance of concrete. In the long term, the gel produced by CSA is used to fill the pores that develop over time, thereby improving the quality of the concrete.

3.4 TOTAL AND CAPILLARY ABSORPTION

The capillary rise absorption tests carried out on the pastes showed that there was an increase in capillary absorption values in the REF pastes compared to the CSA-10% paste, both at 28 days and 91 days of curing (Fig. 7 a-b).

Fig. 7 – Capillary absorption: a) 28 days of curing; and b) 91 days of curing for the REF and CSA-10% pastes

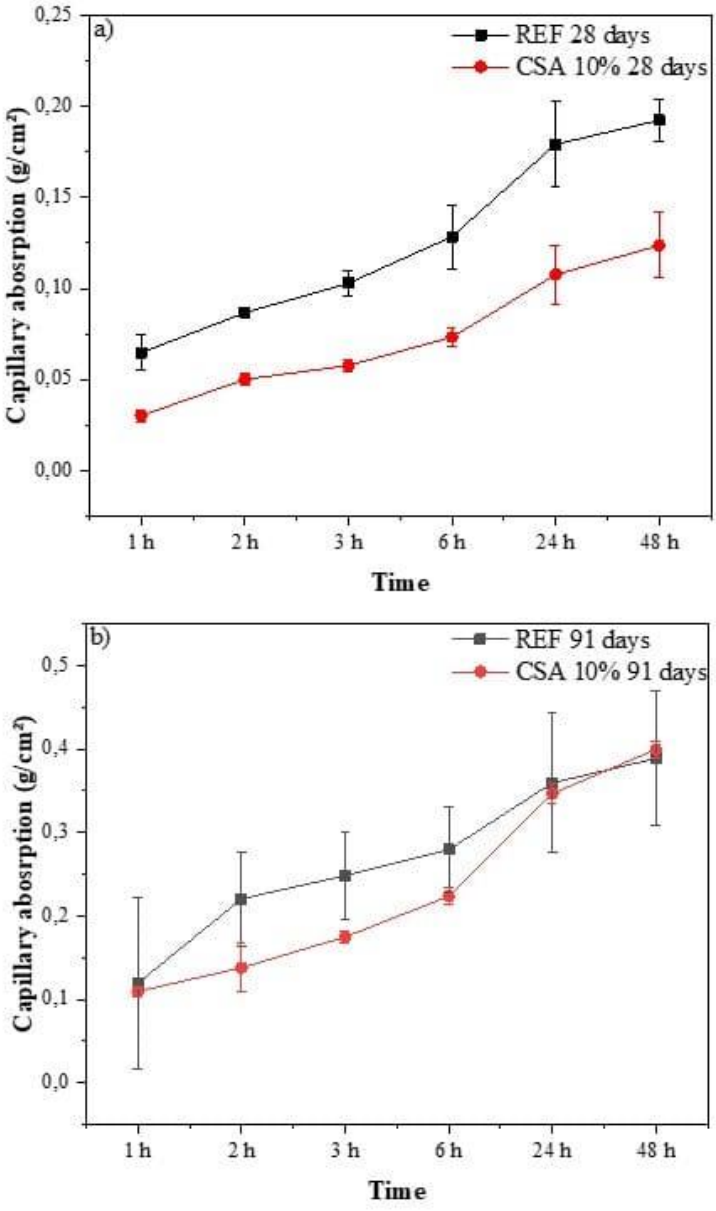

Source: Own authorship (2023).

RC: 148586
Available in: https://www.nucleodoconhecimento.com.br/civil-engineering/corn-straw-ash

The capillary absorption values for the CSA-10% pastes at 28 days were lower. This reduction can be attributed to the smaller pore size in the pastes resulting from the use of ground CSA. However, for the specimens exposed to 91 days of curing during the testing period, a slightly higher capillary absorption value was obtained for the 10% CSA paste compared to the REF. This is because the specimens exhibited cracks when subjected to a lathe.

The reduction in capillary absorption when using CSA is attributed to the pozzolanic reaction, which produces cementitious materials that enhance the bonding properties of the paste. As a result, water penetration into the paste decreases, and cavities are filled (Ahmad *et al*., 2023).

Abubakar *et al*. (2016) mention that an increase in the proportion of corn cob ash and the duration of curing resulted in a reduction in the amount of water absorbed by the manufactured concretes. The same authors also point out that the water absorption values may vary due to inadequate interconnectivity and permeability of the concrete pores, as well as the way in which they are distributed in the mixture.

Comparing the water absorption results of CSA-10% with studies using RHA, it is observed that similar to the findings for corn cob ash, Anto *et al* (2022) conducted an experiment where they substituted 10% of OPC with RHA in a cement paste. The authors discovered that as the curing days progressed, the water absorption decreased. On the other hand, Hu *et al*. (2022) achieved a water absorption rate of 12% when using Portland cement (P.II 52.5) and 10% RHA with a w/c ratio of 0.15. In comparison, the reference sample without RHA had a water absorption rate of 10%. It can be observed that, similar to CSA, the utilization of RHA did not result in a significant increase in water absorption. Even so, it is noteworthy that there is an increase in water absorption with the addition of corn stover ash, as well as a decrease in density as corn stover ash increases (Odeyemi *et al*., 2021; Opeyemi; Otuaga; Oluwasegunfunmi, 2014; Raheem *et al*., 2017).

4. CONCLUSIONS

Given the findings of this research, which aimed to investigate the viability of producing pozzolanic ash from the combustion of corn straw biomass, the following conclusions can be drawn:

- The produced ashes exhibited non-pozzolanic characteristics, along with the presence of alkaline metals, which are detrimental to the strength of the cementitious paste. Consequently, the ash produced at 400 °C, 500 °C, 600 °C, 700 °C, and 800 °C did not show pozzolanic characteristics according to one of the minimum requirements stated in NBR 12653 (ABNT, 2014). This requirement specifies that the sum of SiO_2, Al_2O_3, and Fe_2O_3 should be greater than 50%, and the loss on ignition should be less than 6%. However, the amount of SO_3 remained below the maximum limit of 5%. Even so, it is worth mentioning that even if these do not comply with the standard, other tests are still necessary.

- When observing the mineralogical composition of the samples, it is noted that the XRD patterns of the ashes show deviations in the silica baseline between the Bragg angles of 20° and 40°, indicating the presence of amorphous silica. Furthermore, prominent crystalline peaks of sylvite are observed, supporting the findings from the EDXRF and confirming the presence of KCl in the sample. This presence of KCl contributes to the reduction in compressive strength of the pastes. CSA 800 indicates the formation of other crystalline compounds due to the high temperature, which makes it less reactive than the others.

- The applied grinding procedure was sufficient to reduce the average size of the ash to below 20 μm. Even when using a grinding time of 30 minutes and an average size slightly larger than those used in the literature, satisfactory results were achieved. Pozzolanic activity was observed, indicating that grinding influenced the reactivity of the ash.

- The nitrogen physisorption of the ashes demonstrated that the presence of crystalline silica, specifically quartz, not only impacts the average particle size, which ranges from

6 to 20 μm, but also affects the BET surface area. The highest BET surface area value was obtained for CSA 500 milled for 30 min (D50 = 20.426 μm), resulting in a value of 7757.20 m^2/kg, a pore volume of 0.035 cm^3/g, and a pore diameter of 8.54 nm.

- The pozzolanic activity, as measured by the variation in electrical conductivity and the Chapelle index, indicates that the produced ash has pozzolanic properties. Attention is drawn to the fact that increasing the silica content through thermal processing resulted in a decrease in the pozzolanic activity of the ashes. This is because the carbon content had an impact on the electrical conductivity values. However, the Chapelle pozzolanic activity index showed variation when increasing the ash calcination temperature. The highest value was obtained for CSA 700, with 1056.01 mg $Ca(OH)_2$/g. It should be noted that the CSA 800 experienced a sudden decrease in the Chapelle values. This reduction was attributed to the emergence of new crystalline peaks, which were confirmed by the X-ray diffractogram. Specifically, the presence of cristobalite peaks was observed. Even so, all samples exhibited pozzolanic activity above the minimum value specified in the literature.

- The compressive strength values of the CSA-10% paste showed an increase at the age of 7 days compared to the REF pastes. However, as time passed, the resistance was slightly lower than that of the REF paste. This can be supported by the water absorption values through capillarity, where CPM-10% exhibited an increase in absorption over a 48-hour testing period at 91 days. This phenomenon may be attributed to the pozzolanic activity of the ash in the paste, which results in an increase in pores as the paste ages.

REFERENCES

ABDALLA, L. B.; GHAFOR, K.; MOHAMMED, A. Testing and modeling the young age compressive strength for high workability concrete modified with PCE polymers. **Results in Materials**, v. 1, n. June, p. 100004, 2019.

ABNT - Associação Brasileira de Normas Técnicas. **NBR 12653:** Materiais pozolânicos – Especificação. Rio de Janeiro, Rio de janeiro - Brazil, 2014.

ABNT - Associação Brasileira de Normas Técnicas. **NBR 9778 - Argamassa e concreto endurecidos - Determinação da absorção de água, índice de vazios e massa específica**. Rio de janeiro, Rio de janeiro -Brazil, 2009.

ABNT - Associação Brasileira de Normas Técnicas. **NBR 15895: Materiais pozolânicos – Determinação do teor de hidróxido de cálcio fixado – Método Chapelle modificado**. Rio de Janeiro: 2010.

ABNT - Associação Brasileira de Normas Técnicas. **NBR 16697: Cimento Portland — Requisitos**. Rio de Janeiro, Rio de janeiro - Brazil, 2018.

ABNT - Associação Brasileira de Normas Técnicas. **NBR 9779 - Argamassa e concreto endurecidos — Determinação da absorção de água por capilaridade**. Rio de janeiro, 2012.

ABUBAKAR, I. *et al*. Uniting to end the TB epidemic: Advances in disease control from prevention to better diagnosis and treatment. **BMC Medicine**, v. 14, n. 1, p. 14–17, 2016.

AGWA, I. S. *et al*. Effect of different burning degrees of sugarcane leaf ash on the properties of ultrahigh-strength concrete. **Journal of Building Engineering**, v. 56, n. April, p. 104773, 2022.

AHMAD, J. *et al*. Concrete made with partially substitution corn cob ash: A review. **Case Studies in Construction Materials**, v. 18, n. April, p. e02100, 2023.

ALIU, A. O. *et al*. Evaluation of pozzolanic reactivity of maize straw ash as a binder supplement in concrete. **Case Studies in Construction Materials**, v. 18, n. October 2022, p. e01790, 2023.

ANCA-COUCE, A.; HOCHENAUER, C.; SCHARLER, R. Bioenergy technologies, uses, market and future trends with Austria as a case study. **Renewable and Sustainable Energy Reviews**, v. 135, n. October 2019, p. 110237, 2021.

ANDRADE NETO, J. S. *et al*. Effects of adding sugarcane bagasse ash on the properties and durability of concrete. **Construction and Building Materials**, v. 266, 2021.

ANICIC, B. *et al*. Agglomeration mechanism in biomass fluidized bed combustion – Reaction between potassium carbonate and silica sand. **Fuel Processing Technology**, v. 173, n. June 2017, p. 182–190, 2018.

ANTO, G. *et al*. Mechanical properties and durability of ternary blended cement paste containing rice husk ash and nano silica. **Construction and Building Materials**, v. 342, n. PB, p. 127732, 2022.

BARBOSA, F. L.; CORDEIRO, G. C. Partial cement replacement by different sugar cane bagasse ashes: Hydration-related properties, compressive strength and autogenous shrinkage. **Construction and Building Materials**, v. 272, p. 8–11, 2021.

BARROSO, T. R. **Estudo da atividade pozolânica e da aplicação em concreto de cinzas do bagaço de cana-de-açúcar com diferentes características físico-químicas**. [s.l.] Universidade Estadual do Norte Fluminense Darcy Ribeiro, 2011.

BLOIS, L.; LAY-EKUAKILLE, A. Environmental impacts from atmospheric emission of heavy metals: A case study of a cement plant. **Measurement: Sensors**, v. 18, n. September, p. 1–4, 2021.

CADAVID-GIRALDO, N.; VELEZ-GALLEGO, M. C.; RESTREPO-BOLAND, A. Carbon emissions reduction and financial effects of a cap and tax system on an operating supply chain in the cement sector. **Journal of Cleaner Production**, v. 275, p. 122583, 2020.

CAPABLO, J. *et al*. Ash properties of alternative biomass. **Energy and Fuels**, v. 23, n. 4, p. 1965–1976, 2009.

CHU, Q. *et al*. Bioethanol production: An integrated process of low substrate loading hydrolysis-high sugars liquid fermentation and solid state fermentation of enzymatic hydrolysis residue. **Bioresource Technology**, v. 123, p. 699–702, 2012.

CONAB - Companhia Nacional de Abastecimento. **Série histórica das safras**. 2023. Disponível em: <https://www.conab.gov.br/info-agro/safras/serie-historica-das-safras>.

CORDEIRO, G. C. *et al*. Production of agroindustrial ashes with pozzolanic activity via acid leaching, conjugated burning and ultrafine grinding. **Ambiente Construído**, v. 20, n. 4, p. 189–203, 2020.

CORDEIRO, G. C.; SALES, C. P. Influence of calcining temperature on the pozzolanic characteristics of elephant grass ash. **Cement and Concrete Composites**, v. 73, p. 98–104, 2016.

CORDEIRO, G. C.; TOLEDO FILHO, R. D.; FAIRBAIRN, E. M. R. Effect of calcination temperature on the pozzolanic activity of sugar cane bagasse ash. **Construction and Building Materials**, v. 23, n. 10, p. 3301–3303, 2009.

DANISH; ULUCAK, R. Linking biomass energy and CO_2 emissions in China using dynamic Autoregressive-Distributed Lag simulations. **Journal of Cleaner Production**, v. 250, p. 119533, 2020.

DE GRAZIA, M. T. *et al*. Comprehensive semi-empirical approach to describe alkali aggregate reaction (AAR) induced expansion in the laboratory. **Journal of Building Engineering**, v. 40, n. December 2020, 2021.

EVERETT, D. H.; BUTTERWORTHS, L. International union of pure and applied chemistry (IUPAC) division of physical chemistry. Manual of symbols and terminology for physicochemical quantities and units . Appendix II: Definitions, Terminology and Symbols in Colloid and Surface Chemistry PART . n. July, p. 579–638, 1972.

HASNAIN, M. H. *et al*. Eco-friendly utilization of rice husk ash and bagasse ash blend as partial sand replacement in self-compacting concrete. **Construction and Building Materials**, v. 273, p. 121753, 2021.

HU, L. *et al*. Effect of rice husk ash on carbon sequestration, mechanical property and microstructure evolution of cement-based materials with early-age carbonation treatment. **Cement and Concrete Composites**, v. 133, n. December 2021, p. 104672, 2022.

JIN, J. *et al*. Cumulative effects of bamboo sawdust addition on pyrolysis of sewage sludge: Biochar properties and environmental risk from metals. **Bioresource Technology**, v. 228, p. 218–226, 2017.

KANG, Y. *et al*. Bioenergy in China: Evaluation of domestic biomass resources and the associated greenhouse gas mitigation potentials. **Renewable and Sustainable Energy Reviews**, v. 127, n. April, p. 109842, 2020.

KANTRO, D. Influence of Water-Reducing Admixtures on Properties of Cement Paste—A Miniature Slump Test. **Cement, Concrete and Aggregates**, v. 2, n. 2, p. 95–102, 1980.

LIMA, C. P. F. DE; CORDEIRO, G. C. Evaluation of corn straw ash as supplementary cementitious material: Effect of acid leaching on its pozzolanic activity. **Cement**, v. 4, n. July 2020, p. 100007, 2021.

LUXAN M P; MADRUGA F; SAAVEDRA J. Rapid Evaluation of Pozzolanic Activity of Natural Products. **Cement and Concrete Research**, v. 19, p. 63–68, 1989.

MARTIRENA, F.; MONZÓ, J. Vegetable ashes as Supplementary Cementitious Materials. **Cement and Concrete Research**, v. 114, n. November 2016, p. 57–64, 2018.

MENGI-DINÇER, H.; EDIGER, V.; YESEVI, G. Evaluating the International Renewable Energy Agency through the lens of social constructivism. **Renewable and Sustainable Energy Reviews**, v. 152, n. May, p. 111705, 2021.

MO, K. H. *et al*. Green concrete partially comprised of farming waste residues: A review. **Journal of Cleaner Production**, v. 117, p. 122–138, 2016.

MOTA, L. C. S. *et al*. Avaliação dos efeitos da adição de carvão ativado residual ao concreto. ANAIS DO 59º CONGRESSO BRASILEIRO DO CONCRETO – 59CBC2017. **Anais[...]** Bento Gonçalves-RS: 2017.

NIU, Y. *et al*. Effects of water leaching (simulated rainfall) and additives (KOH, KCl, and SiO_2) on the ash fusion characteristics of corn straw. **Applied Thermal Engineering**, v. 154, n. September 2018, p. 485–492, 2019.

ODEYEMI, S. O. *et al*. Effect of combining maize straw and palm oil fuel ashes in concrete as partial cement replacement in compression. **Trends in Sciences**, v. 18, n. 19, p. 1–11, 2021.

OLIVEIRA, I. J. *et al.* Recomendações técnicas para o cultivo do milho no Amazonas. **Embrapa. Circular Técnica 68**, p. 28, 2018.

OPEYEMI, D. A.; OTUAGA, M. P.; OLUWASEGUNFUNMI, V. Synergic Effect of Maize Straw Ash and Rice Husk Ash on Strength Properties of Sandcrete. **European Journal of Basic and Applied Sciences**, v. 1, n. 1, 2014.

PAIVA, O. A. **Durabilidade de concretos contendo cinza do bagaço da cana-de-açucar**. [s.l.] Universidade Federal do Rio de Janeiro, 2016.

PERNÁ, I. *et al*. The synthesis and characterization of geopolymers based on metakaolin and high LOI straw ash. **Construction and Building Materials**, v. 228, 2019.

PINHEIRO, S. C. **Influência de sílica gel e de partículas micro e submicrométricas produzidas a partir da cinza do bagaço de cana-de-açúcar na hidratação e estrutura de poros de pastas de cimento**. [s.l.] Universidade Federal do Rio de Janeiro, 2015.

PINO, M. S. *et al*. Bioreactor design for enzymatic hydrolysis of biomass under the biorefinery concept. **Chemical Engineering Journal**, v. 347, n. March, p. 119–136, 2018.

QI, T.; FENG, G.; WANG, H. **Pozzolanic Activity of Corn Straw Leaf Ash Produced at Different Temperatures and Treated with Portlandite Solution**. BioResources, 2020.

QUDOOS, A. *et al*. Performance evaluation of the fiber-reinforced cement composites blended with wheat straw ash. **Advances in Materials Science and Engineering**, v. 2019, 2019.

G. DE AZEVEDO, A. *et al*. Possibilities for the application of agro-industrial wastes in cementitious materials: A brief review of the Brazilian perspective. **Cleaner Materials**, v. 3, n. October 2021, p. 100040, 2022.

RAHEEM, A. A. *et al*. Application of corn stalk ash as partial replacement for cement in the production of interlocking paving stones. **International Journal of Engineering Research in Africa**, v. 30, p. 85–93, 2017.

RAVERDY, M. *et al*. Appreciation de l'activite pouzzolanique des constituants secondaires. 7th Int. Congr. Chem. Cem. Paris. **Anais[...]** 1980.

ROLÓN, B. G.; CASTAÑEDA, P. F. Mechanical resistance and corrosion of concrete added with ashes of corn, sorghum, and wheat. **Cleaner Materials**, v. 2, n. November, p. 1–11, 2021.

SING, K. S. W. *et al*. Reporting physisorption data for gas/solid systems with special reference to the determination of surface area and porosity. **Pure Appl. Chem**, v. 57, n. 4, p. 603–619, 1985.

STATISTA. **Global corn production in 2021/2022, by country**. [s.d.]. Disponível em: <https://www.statista.com/statistics/254292/global-corn-production-by-country/>.

THENG, D. *et al*. All-lignocellulosic fiberboard from corn biomass and cellulose nanofibers. **Industrial Crops and Products**, v. 76, p. 166–173, 2015.

TITILOYE, J. O.; ABU BAKAR, M. S.; ODETOYE, T. E. Thermochemical characterisation of agricultural wastes from West Africa. **Industrial Crops and Products**, v. 47, p. 199–203, 2013.

UN ENVIRONMENT AND INTERNATIONAL ENERGY AGENCY. **Towards a zero-emission, efficient, and resilient buildings and construction sector.** [s.l: s.n.] 2017. Disponível em: <https://www.worldgbc.org/news-media/global-status-report-2017>.

VIEIRA, A. P. *et al*. Effect of particle size, porous structure and content of rice husk ash on the hydration process and compressive strength evolution of concrete. **Construction and Building Materials**, v. 236, p. 117553, 2020.

WANG, H. *et al*. Effect of partial substitution of corn straw fly ash for fly ash as supplementary cementitious material on the mechanical properties of cemented coal gangue backfill. **Construction and Building Materials**, v. 280, p. 122553, 2021.

XU, Y. *et al*. Effect of the ash melting behavior of a corn straw pellet on its heat and mass transfer characteristics and combustion rate. **Fuel**, v. 286, n. P2, p. 119483, 2021.

YAO, X. *et al*. Experimental investigation of physicochemical and slagging characteristics of inorganic constituents in ash residues from gasification of different herbaceous biomass. **Energy**, v. 198, p. 117367, 2020.

YAO, X.; XU, K.; LIANG, Y. Comparative Analysis of the Physical and Chemical Properties of Different Biomass Ashes Produced from Various Combustion Conditions. **BioResources**, v. 12, n. 2, p. 3222–3225, 2017.

ZENG, X.; MA, Y.; MA, L. Utilization of straw in biomass energy in China. **Renewable and Sustainable Energy Reviews**, v. 11, n. 5, p. 976–987, 2007.

ZHAO, X. *et al*. Insight into the influence of water leaching on ash fusion behavior and alkali metal migration for corn and rice straw. **Journal of the Energy Institute**, v. 110, n. February, p. 101362, 2023.

ZHAO, Y. *et al*. Bioethanol from corn stover – Integrated environmental impacts of alternative biotechnologies. **Resources, Conservation and Recycling**, v. 155, n. November 2019, p. 104652, 2020.

ZHOU, H. *et al*. Syngas composition and ash characteristics of corn straw under a CO_2 atmosphere. **Biomass and Bioenergy**, v. 166, n. September, p. 106630, 2022.

Submitted: September 20, 2023.

Approved: September 21, 2023.

[1] Advisor. Doctorate, Master's and Bachelor's degrees in Civil Engineering. ORCID: 0000-0002-5364-3443. Currículo Latte: http://lattes.cnpq.br/9802998425503349.
[2] Doctorate, Master's and Bachelor's degrees in Civil Engineering. ORCID: 0009-0008-7816-2620. Currículo Latte: http://lattes.cnpq.br/9802998425503349.
[3] Master in Materials Science and Engineering and Degree in Civil Engineering. ORCID: 0000-0002-2617-4485. Currículo Latte: http://lattes.cnpq.br/7400275080422973.
[4] Master's student in Materials Science and Engineering at the Federal University of São Carlos (UFSCar) – SP, Civil Engineer at the State University of Amazonas (UEA) – AM. ORCID: 0000-0002-9702-9488. Currículo Latte: http://lattes.cnpq.br/1748736510715140.
[5] Civil Engineering student. ORCID: 0009-0003-1577-2062. Currículo Latte: http://lattes.cnpq.br/4769057271599546.
[6] Doctorate, Master's degree and Bachelor's degree in Civil Engineering. ORCID: 0000-0002-2140-6208. Currículo Latte: http://lattes.cnpq.br/5473986728624292.